Observability of Ischemia and the Need for Patient Specific Geometrical Models in Inverse ECG

Glenn T Lines[1,2,3], Marius Lysaker[1,3,4] , Bjørn F Nielsen[1,3,5]

[1] Simula Research Laboratory, Oslo, Norway
[2] Department of Informatics, University of Oslo, Oslo, Norway
[3] Center for Cardiological Innovation, Oslo University Hospital, Oslo, Norway
[4] Telemark University College, Porsgrunn, Norway
[5] Department of Mathematical Sciences and Technology,
Norwegian University of Life Sciences, Ås, Norway

Abstract

We have performed ECG simulations on four realistic geometries in order to quantify the effect of ischemic location in the left ventricle in terms of ST shifts in the body surface potential (BSP). Using 64 electrodes we found that most segments were clearly visible on at least some of the electrodes, although signals were generally weaker from the left side of the heart. We also found that cancelling effects can occur when more than one ischemic area is present.

Significant inter-patient difference where observed, demonstrating the need for patient specific geometries. Within groups of similar body type the results were highly correlated, indicating that it is probably enough to use approximative geometries.

1. Introduction

Non ST-elevation ischemia (NSTEMI) can by definition not be detected by ST shifts using the standard 12 lead ECG. The non-observability of NSTEMI can be due to the size or the placement of the ischemia, or due to canceling effects. In this work we use the bidomain framework to do a theoretical analysis on the observability using an ECG vest with 64 electrodes.

2. Methods

We have computed the ST shift on the torso in response to an ischemic heart. The simulation framework is similar to the procedure found in [1]. Using the bidomain framework [2], the transmembrane potential (v) and the extra cellular potential (u) are related as follows:

$$\nabla \cdot ((M_i + M_e)\nabla u) = -\nabla \cdot (M_i \nabla v) \qquad (1)$$

where M_i and M_e are conductivity tensors in the intra cellular and extra cellular space, respectively.

We only consider the PR interval and the ST interval. In both phases the membrane potential is approximated by a piecewise constant function, which has one value in the ischemic part of the tissue and another in the healthy part of the tissue.

Since (1) is linear we can also use the equation to compute the observed shift in u by supplying the shift in v rather than v itself. In the healthy part of the tissue there will be no shift, while there will be a negative shift in v in the ischemic areas, representing the decreased action potential amplitude in this area. See [1] for further details. Given u on the heart surface, the body surface potential is computed using FE model of the torso. Four geometries were used in this study, three patients and one healthy volunteer. See [3] for the details on geometry construction.

The left ventricle was divided into 60 segments, as shown in Figure 1. An ischemic situation was simulated for each segment and the corresponding ST shift computed at 64 locations at the body surface, see Figure 2. We have subtracted the Wilson central terminal potential from the body surface potential, so the value at the chest leads is comparable to the chest leads of a standard ECG.

For each patient we thus have a matrix of virtual BSP measurements: B_{ij}^k, with $k = 1, \ldots, 4$ denoting the patient number, $i = 1, \ldots, 64$ the electrode, and $j = 1, \ldots, 60$ the ischemic segment.

3. Results

For each patient we get a simulated BSP for each segment in the LV. For example, the ST shift generated by an ischemia in Segment 3 is shown in the left panel of Figure 3. This results in an ST depression (blue) in the chest leads.

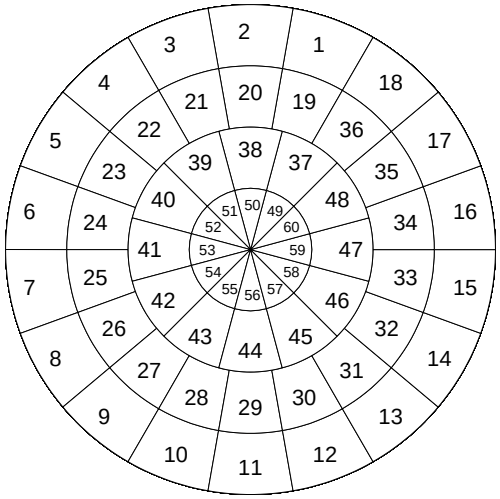

Figure 1. Numbering scheme of the bulls eye plot of the left ventricle. Segments 1 to 18 are basal, 49 to 60 are apical. Top of the figure is anterior, bottom is posterior. Segments to left on the figure are on the septal wall.

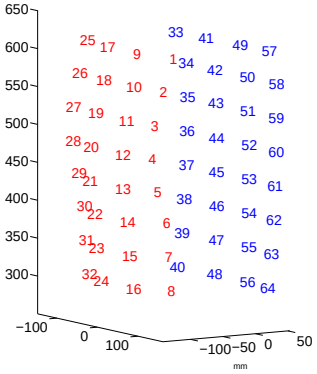

Figure 2. Locations of body surface electrodes. 32 are located on the front (red), and 32 on the back (blue).

3.1. Observability at the body surface

We have performed similar simulations for all 60 segments and as an example the ST shift seen in Electrode 12 is shown in the right panel of Figure 3. As already evident from the left panel we get an ST depression from Segment 3 in this electrode. Overall we see that ischemic areas in the left side of the heart generates ST elevation, while ischemia on the septal wall leads to ST depression in this electrode (blue areas). We can also note that there are segments for which an ischemic area will not show up on this electrode (the green areas).

We can repeat the procedure for the remaining electrodes to get a complete view of how the relationship between the ischemic location and the corresponding ST shift. Figure 4 show the results for the front electrodes, 1-32.

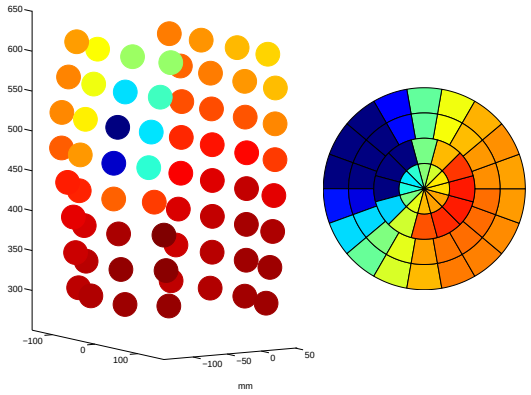

Figure 3. Left: ST shift in response to ischemia in Segment 3 (see Figure 1). Red is ST elevation, blue is ST depression. Right: ST shift in electrode number 12 (see Figure 2) in response to the 60 different ischemic cases.

As expected the strongest signal is on the electrode closest to the heart. For all electrodes there are ischemic segments that does not result in an ST shift (green color). But there are no segments that are silent over all electrodes, so in that sense the BSPM *sees* the whole ventricle. This is illustrated for patient 3 in the right panel of Figure 5. Ischemia in the left part of the heart generates a weaker signal, but not lower than 40% of the median signal strength.

Cancelling effects are possible though. For example, if both segment 19 and 28 are ischemic, the resulting ST shift is small over all electrodes (not shown).

3.2. Patient specific variations

The results above was derived using a single patient geometry. If we can show that the situation shown in Figure 4 is the same regardless of patient geometry we could conclude that there is in fact no need for patient specific geometries as there would be a robust relationship between ischemic region and the BSPM response. In order to investigate this we have made maps as in Figure 4 for all four patients. Correlation coefficients between patients were then calculated for each segments using all electrodes. The table below shows how the average correlation coefficients varied between the four patients:

	2	3	4
1	0.73	0.82	0.74
2		0.88	0.64
3			0.76

There is quite a range in values. The highest correlation is between number 2 and 3 at 0.88. The lowest is between 2 and 4 at 0.64. Overall patient 4 stands out as less correlated with the rest of the group compared to internal correlation within the 1-3 group. This is consistent with the fact that

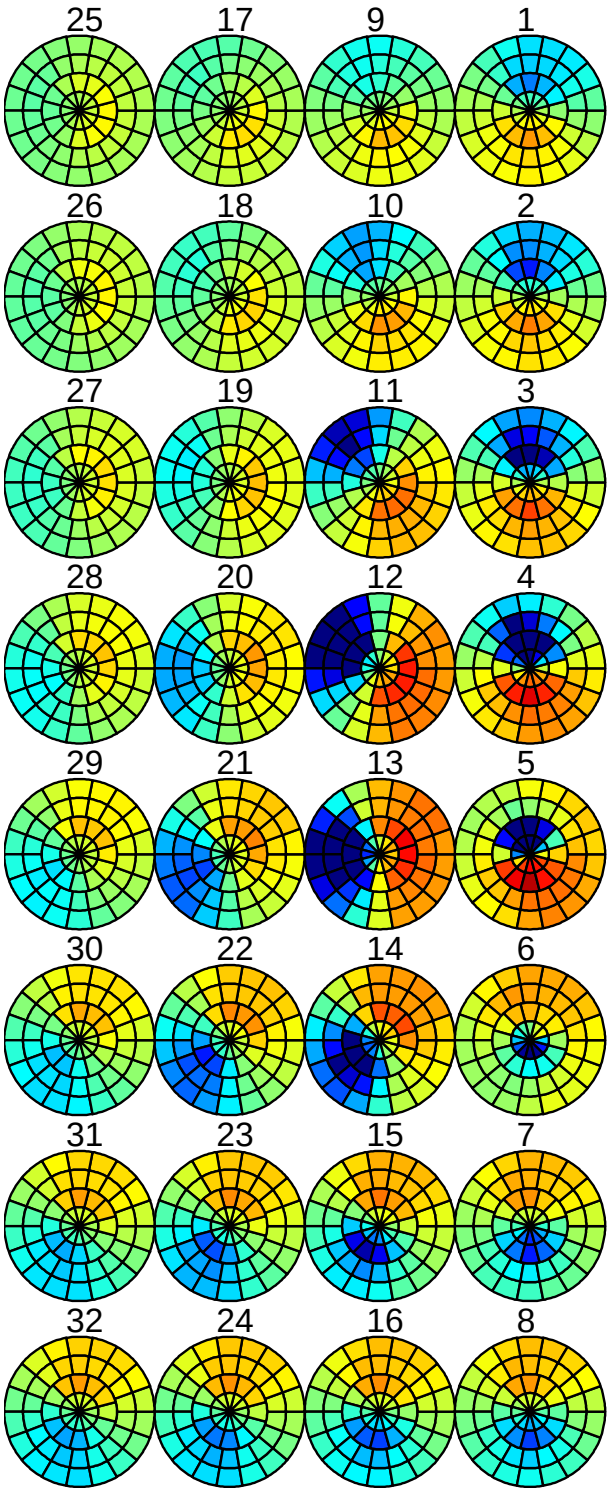

Figure 4. ST shifts on chest side electrodes in response to ischemic location.

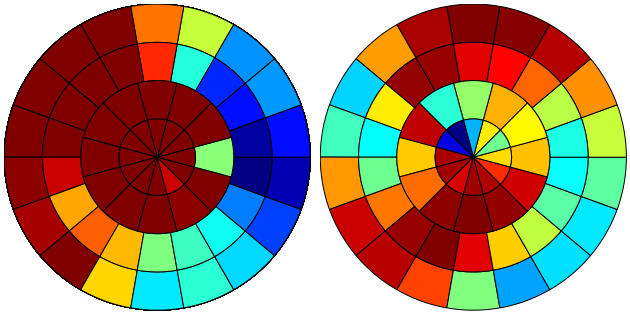

Figure 5. Left: Maximum amplitude over all electrodes. Dark red corresponds to above median strength in signal, while deep blue corresponds to a signal strength of 40% of the median. Right: Correlation of BSPM signals from patient 2 and 4. Deep blue: Least correlation, 0.3. Deep red: Most correlation, 0.8.

number 4 was the volunteer, a person of normal weight, while 1-3 are actual patients that were either overweight or obese.

The average 0.64 might not say much in itself, and from our point of view the segments with the least correlation represents the critical cases, where the risk would be the greatest to wrongly identify an ischemic segment. The right panel of Figure 5 shows the correlation coefficients between patient 2 and 4 as a bulls-eye plot. The range between is from $\rho \in [0.3, 0.8]$. The lowest correlation, i.e. the most dissimilar BSPMs, occurs for segment 51. To illustrate the value $\rho = 0.3$ we show in the top panel of Figure 6 the BSPM for this case. For both patients we see ST elevation most places, and a very localized ST depression on the chest. The relatively low correlation is due to fact the area of depression is slightly shifted between the two cases.

Conversely, can two different segments give rise to very similar BSPMs? The lower panel of Figure 6 gives an illustration of this where Segment 14 in Patient 2 and Segment 59 in Patient 4 gives very similar results. These segments are on the same side of the heart, but one is basal while the other is apical. This indicates that the geometries in this case are too dissimilar to be used in place of each other.

Figure 7 shows the correlation between of BSPMs for all possible combinations of ischemic segments. As expected the correlation along the diagonal is high. There are also periodic off-diagonal bands, arising from segments that are in negibourings bands. For example, Segment 8 for Patient 4 is expected to not only be correlated with the same segment in Patient 2, but also to be correlated with the segments 26, 42 and 54, as these are similarly located, only differing in apical distance, c.f. Figure 1. What we infact see in this case is that there is a slight offset compared to this expectation, indicative of a relative rotation between the hearts.

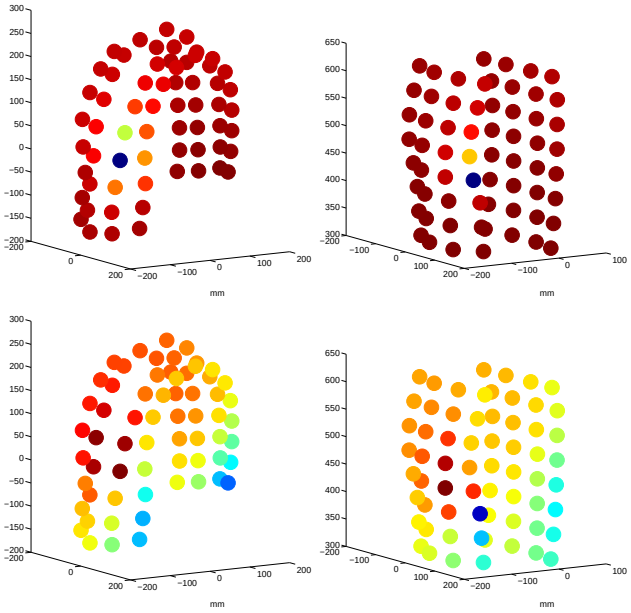

Figure 6. BSPM for Patient 2 (left) and 4 (right). Top panel: Segment 51 for both, but only $\rho = 0.3$. Lower panel: Different segments (no. 14 for left, no. 59 for right), but still high correlation, $\rho = 0.9$.

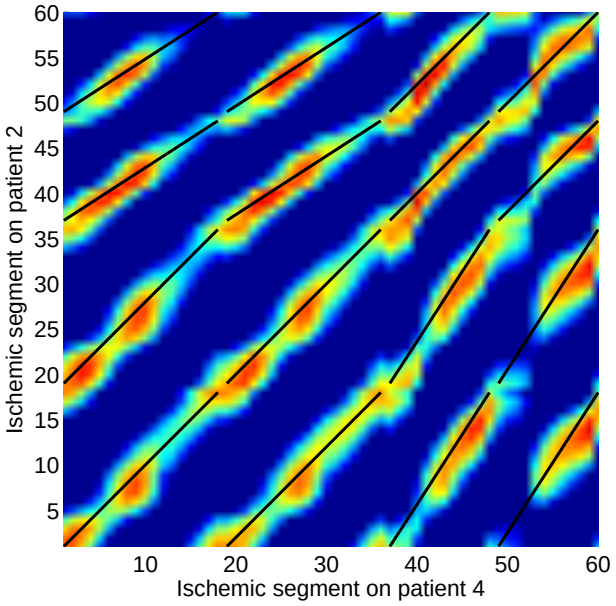

Figure 7. Correlation between BSPMs. The black line represents corresponding ventricular position, see Figure 1.

4. Conclusions

As expected, the chest leads provided most information. Furthermore, there were clear similarities between patients with respect to ischemic location and response in the body surface potential. However, the simulations also revealed significant differences in response, with average correlation coefficients in the range 0.64-0.88. It seems likely that body shape must be taken into account for precise inverse solution, but that an exact match of patient geometry is probably not necessary.

Using all 64 leads there were no ventricular segments that where silent, however the left part of heart displayed weaker signals. Also examples of canceling effects were observed, were opposing segments would lead to a very small ST shift on the body surface.

Acknowledgements

We would like to thank Kristina Hermann Haugaa, Andreas Abildgaard and Jan Gunnar Fjeld at Oslo University Hospital and Per Grøttum at Faculty of Medicine, University of Oslo for providing us with the clinical data that was used in this study.

References

[1] Lysaker M, Nielsen B, Grøttum P. On the use of bidomain model for computing the position and size of ischemic regions; a validation study. Computing in Cardiology 2012; 39:449–452.

[2] Henriquez C. Simulating the electrical behavior of cardiac tissue using the bidomain model. Critical Reviews in Biomedical Engineering 1993;21(1):1–77.

[3] Nielsen B, Lysaker M, Grøttum P. Computing ischemic regions in the heart with the bidomain model - first steps towards validation. IEEE Transactions on Medical Imaging 2013;32(6):1085–1096.

Address for correspondence:

Glenn T. Lines
Simula Research Laboratory
P.O.Box 134, 1325 Lysaker, Norway
glennli@simula.no